

Implementation of a Robust Algorithm for Prediction of Forming Limit Diagrams

M. Ganjani and A. Assempour

(Submitted June 4, 2006; in revised form October 30, 2006)

In this article, a robust algorithm for prediction of forming limit diagrams (FLD) has been presented. The presented model is based on the “Marciniak and Kuczynski” (M-K) theory. Solution to the system of equations has been obtained by applying the Newton’s method. Since the Newton’s method usually has nonconverging problem, a particular backtracking algorithm has been developed and applied. In this algorithm, a technique for step length selection in the frame of gradient descent method has been implemented. Also for the convergence criterion the so-called “Armijo” condition has been used. For verification of the results, BBC2000 yield function and Swift hardening law for AK steel metal have been used. To obtain the necking angle, the effect of groove orientation on the left- and right-hand sides of FLD has been considered. Finally, the predicted FLD has been compared with the published experimental results.

Keywords backtracking, BBC2000 yield function, convergence, forming limit diagrams, Newton’s method

List of symbols

σ	Cauchy stress tensor
σ_1, σ_2	principal stress components
$\sigma_{nn}, \sigma_{tt}, \sigma_{nt}$	stress components in the groove coordinate
$\bar{\sigma}_Y$	effective stress obtained from hardening law
$\bar{\sigma}_y$	effective stress obtained from yield function
ε_0, K, n, m	material constants
a, b, c, M, N, P, Q, R	material constants
$\bar{\varepsilon}, \dot{\bar{\varepsilon}}$	effective plastic strain and its rate
$d\bar{\varepsilon}$	effective plastic strain increment
$d\varepsilon$	strain increment tensor
$d\varepsilon_{nn}, d\varepsilon_{tt}, d\varepsilon_{nt}$	strain increments in the groove coordinates
$d\varepsilon_1, d\varepsilon_2, d\varepsilon_3$	strain increments in the material coordinates
α	ratio of stresses along the strain path
ρ	ratio of strain increments along the strain path
\mathbf{T}	rotation matrix
$d\lambda$	plastic multiplier
F_{nn}, F_{nt}	force equations in the groove directions
f	inhomogeneous factor
δx	Newton’s step
\mathbf{J}	Jacobian matrix
θ	angle between the groove coordinates and the material coordinates
λ	Newton’s step length

1. Introduction

Theoretical studies in the analysis of sheet metal failures are referred in the forming limit diagrams (FLD) which were first

M. Ganjani and A. Assempour, Center of Excellence in Design, Robotics and Automation, Department of Mechanical Engineering, Sharif University of Technology, Azadi Avenue, P.O. Box 11365-9567, Tehran, Iran. Contact e-mail: assem@sharif.edu.

conceptually introduced by Keeler (Ref 1) and Goodwin (Ref 2). Generally these diagrams represent the limit strains that a sheet can resist against the splitting. Since extracting the FLD experimentally is cost and time consuming. Many researchers have tried to obtain these diagrams theoretically. Marciniak and Kuczynski (M-K) (Ref 3, 4) developed a FLD model for localized necking which contains an initial thickness imperfection in the form of a groove. This model is a perfect method for prediction of FLD. Based on this model, the effects of yield functions have been studied by several authors. Slota and Spisak (Ref 5) used Hill’s 1993 yield function. Banabic et al. (Ref 6) used BBC2003 yield function in M-K model. Banabic and Dannenmann (Ref 7) used the Hill’s 1993 and M-K model for the calculation of the limit strains. Huang et al. (Ref 8) used Hill’s quadratic anisotropic yield criterion. Kuroda and Tvergaard (Ref 9) investigated the influence of different orthotropic yield functions in the M-K model. Cao et al. (Ref 10) predicted localized thinning of sheet metal using Karafillis and Boyce yield function based on the M-K model.

In the process of prediction of FLD by M-K method, the system of equations basically consists of equilibrium, compatibility, and energy balance equations. These equations are composed of some variables which are mainly the stress and strain components. To simplify the numerical solution, some researchers used only the equilibrium equations and Runge-Kutta numerical method (Ref 11, 12). For the system of equations with more than one variable, the Runge-Kutta numerical method will no longer be valid. For such cases, usually the Newton’s method is more applicable. In most cases, several researchers applied the Newton’s method for only two equilibrium equations (Ref 10, 13). Some authors used the compatibility and yield surface equations with application of Newton’s method (Ref 14, 15). However, in all these cases, sometimes Newton’s method shows nonconverging problem. Thus using this method alone in the solution does not guarantee the robustness of the algorithm.

In this article, the M-K model with Newton’s method has been applied for prediction of FLD. The complete system of equations including four variables has been considered. To

guarantee the convergence of solution, a particular backtracking technique has been included in the Newton's method. The technique has shown significant influence on the converging of the results. Also the so-called "BBC2000" yield function has been considered in the system of equations. The procedure has been applied for prediction of FLD in AK steel and the results have been compared with the published experimental results.

2. Marciniak and Kuczynski Model

In this article, calculations of limit strains are based on "Marciniak and Kuczynski" (M-K) (Ref 3) theory. In this model, it has been assumed that there is a narrow groove in the surface. Thus the sheet is composed of a safe area and a groove area which are denoted by "a" and "b", respectively. This groove leads to localized necking in the sheet (see Fig. 1). For modeling the groove, an imperfection factor is introduced which represents the thickness ratio $f = t_b/t_a$, where "t" denotes the thickness. Imposing of stress components at rolling and transverse directions in the safe area causes the progression of strain increments in both the safe and groove areas.

Necking occurs when the effective strain in the groove area is 10 times of that in the safe area (Ref 10, 13-15). During the entire process, the force equilibrium equations at groove direction must be satisfied as follows:

$$\begin{aligned} F_{nt}^a &= F_{nt}^b \\ F_{nn}^a &= F_{nn}^b \end{aligned} \quad (\text{Eq 1})$$

Here F_{nn} and F_{nt} are forces in the normal and tangential directions in the groove. By introducing the stress state in these areas, Eq 1 could be rewritten as follows:

$$\begin{aligned} \sigma_{nt}^a \exp(\varepsilon_3^a) t_0^a &= \sigma_{nt}^b \exp(\varepsilon_3^b) t_0^b \\ \sigma_{nn}^a \exp(\varepsilon_3^a) t_0^a &= \sigma_{nn}^b \exp(\varepsilon_3^b) t_0^b \end{aligned} \quad (\text{Eq 2})$$

where σ_{nn} and σ_{nt} are stress components in the "n" and "t" directions, t_0^a and t_0^b are initial thicknesses in the safe and groove regions, respectively. Imperfection factor f can be expressed as a function of the initial defect:

$$f = f_0 \exp(\varepsilon_3^b - \varepsilon_3^a) \quad (\text{Eq 3})$$

Herein f_0 is the initial imperfection factor and denoted by t_0^b/t_0^a , and ε_3 is the strain in thickness direction calculated by incompressibility condition:

$$\varepsilon_3 = -(\varepsilon_1 + \varepsilon_2) \quad (\text{Eq 4})$$

Thus, force equilibrium conditions are summarized as follows:

$$\begin{aligned} f \sigma_{nn}^b &= \sigma_{nn}^a \\ f \sigma_{nt}^b &= \sigma_{nt}^a \end{aligned} \quad (\text{Eq 5})$$

It is assumed that the strain increments parallel to the groove are the same in both regions:

$$d\varepsilon_{tt}^b = d\varepsilon_{tt}^a \quad (\text{Eq 6})$$

Using flow rule, the strain increment components are related to the effective strain increment and stress state as follows:

$$d\varepsilon_{ij} = d\bar{\varepsilon} \frac{\partial \bar{\sigma}_y}{\partial \sigma_{ij}} \quad (\text{Eq 7})$$

Thus, the unknown parameters in the groove zone are stress components $\sigma_{nn}^b, \sigma_{tt}^b, \sigma_{nt}^b$ and effective strain increment $d\bar{\varepsilon}^b$.

3. System of Equations

For calculating the limit strains, it is required to calculate the strain and stress components in the safe region. This region is loaded under constant stress relation with the ratio α . For this purpose, a value for α between 0 and 1 is selected and this value must remain constant at entire time during each loading stage. At starting, a small value for effective strain increment $d\bar{\varepsilon}_a$ (for example 0.0001) is selected. Substituting the effective strain in the hardening law, the effective stress $\bar{\sigma}_y$ is obtained. Since the effective stresses from hardening law and yield function must be equal, σ_x^a and σ_y^a can be obtained. A relationship between effective strain and effective stress is represented by the Swift relation:

$$\bar{\sigma}_y = K(\varepsilon_0 + \bar{\varepsilon})^n (\dot{\bar{\varepsilon}})^m \quad (\text{Eq 8})$$

where K is the strength coefficient, ε_0 the pre-strain, n the hardening law exponent and m is the strain rate sensitivity. Using the assumed $d\bar{\varepsilon}_a$ in the flow rule, stress and strain components are calculated. Using the rotation matrix, \mathbf{T} , the strain and stress tensors are transformed to the groove system of coordinates:

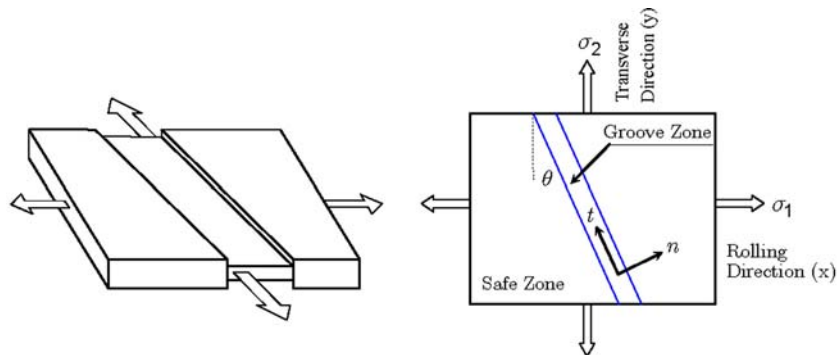


Fig. 1 Schematic of the M-K model on prediction of FLD

$$\begin{aligned}\sigma^{ntz} &= \mathbf{T} \sigma^{xyz} \mathbf{T}^T \\ &= \begin{bmatrix} \sigma_{nn} & \sigma_{nt} \\ \sigma_{nt} & \sigma_{tt} \end{bmatrix}\end{aligned}\quad (\text{Eq 9})$$

with,

$$\mathbf{T} = \begin{bmatrix} \cos(\theta) & \sin(\theta) \\ -\sin(\theta) & \cos(\theta) \end{bmatrix} \quad (\text{Eq 10})$$

The unknown parameters in the groove region can be defined by the variable vector \mathbf{x} as

$$\mathbf{x} = [\sigma_{nn}^b \quad \sigma_{tt}^b \quad \sigma_{nt}^b \quad d\bar{\epsilon}_b]^T \quad (\text{Eq 11})$$

Using the compatibility and force equilibrium conditions, three equations for the vector of functions are obtained. In this article, the energy relation is used as Eq (4):

$$d\epsilon_{nn}^b \sigma_{nn}^b + d\epsilon_{tt}^b \sigma_{tt}^b + d\epsilon_{nt}^b \sigma_{nt}^b = d\bar{\epsilon}_b \bar{\sigma}_Y \quad (\text{Eq 12})$$

Thus, vector of functions, \mathbf{F} is introduced as follows:

$$\mathbf{F} = [F_1 \quad F_2 \quad F_3 \quad F_4]^T \quad (\text{Eq 13})$$

where

$$F_1 = \frac{d\epsilon_{nn}^b \sigma_{nn}^b + d\epsilon_{tt}^b \sigma_{tt}^b + d\epsilon_{nt}^b \sigma_{nt}^b}{d\bar{\epsilon}_b \bar{\sigma}_Y} - 1 = 0 \quad (\text{Eq 14})$$

$$F_2 = \frac{d\epsilon_{tt}^b}{d\epsilon_{tt}^a} - 1 = 0 \quad (\text{Eq 15})$$

$$F_3 = f \frac{\sigma_{nn}^b}{\sigma_{nn}^a} - 1 = 0 \quad (\text{Eq 16})$$

$$F_4 = f \frac{\sigma_{nt}^b}{\sigma_{nt}^a} - 1 = 0 \quad (\text{Eq 17})$$

Localized necking in sheet metal is caused when the equivalent strain increment in groove zone becomes 10 times of that in the safe region. Calculation of limit strains is repeated for different values of θ between 0° and 90° . For such calculation, the following formula is used:

$$\tan(\theta + d\theta) = \frac{1 + d\epsilon_1^a}{1 + d\epsilon_2^a} \tan(\theta) \quad (\text{Eq 18})$$

Minimum value of major localization strain is selected among the calculation loops by variation of θ . The selected minimum strain for any value of α is used in the FLD.

4. Application of Newton's Method

There are several common methods for finding the root of a general nonlinear equation $f(x) = 0$. Bisection, false position, secant, Bus and Dekker, and Newton-Raphson methods are some of the examples (Ref 16). Based on comparisons between these methods (Ref 16), the best technique for solving system of nonlinear equations is Newton's method. Thus in the present work, this method has been adopted and its implementation is briefly discussed as the following. Consider N functions F_i involving variables x_i , $i = 1, 2, \dots, N$ as follow:

$$F_i(x_1, x_2, \dots, x_N) = 0 \quad i = 1, 2, \dots, N. \quad (\text{Eq 19})$$

By using Taylor series, functions F_i can be expanded as follows:

$$\mathbf{F}(\mathbf{x} + \delta\mathbf{x}) = \mathbf{F}(\mathbf{x}) + \mathbf{J} \cdot \delta\mathbf{x} + O(\delta\mathbf{x}^2) \quad (\text{Eq 20})$$

where \mathbf{J} is the matrix of partial derivatives and is called the "Jacobian" matrix.

$$J_{ij} = \frac{\partial F_i}{\partial x_j} \quad (\text{Eq 21})$$

By neglecting terms of order $\delta\mathbf{x}^2$ and higher and by setting $F(\mathbf{x} + \delta\mathbf{x}) = 0$, one obtains set of nonlinear equations:

$$\mathbf{J} \cdot \delta\mathbf{x} + \mathbf{F} = 0 \quad (\text{Eq 22})$$

or,

$$\delta\mathbf{x} = -\mathbf{J}^{-1} \cdot \mathbf{F} \quad (\text{Eq 23})$$

Then, the variable $\delta\mathbf{x}$ is added to the solution vector:

$$\mathbf{x}_{\text{new}} = \mathbf{x}_{\text{old}} + \delta\mathbf{x} \quad (\text{Eq 24})$$

To exit the Newton's calculation loops, it is required to define a criterion. In the present formulations, there exists a vector of function which has four components. All components of this vector have the same important rank. Thus, the maximum value among these components has been selected to be compared with the tolerance in the Newton's loop, i.e.

$$\|\mathbf{F}\|_\infty = \max_{i=1}^4 |F_i| \quad (\text{Eq 25})$$

this is called ∞ -norm.

5. Convergence Criterion

The convergence of Newton's method significantly depends on the initial guess. If the initial guess is not sufficiently close to the root, Newton's method for solving nonlinear equations is not successful. Figure 2 depicts the state of nonconverging situation in the Newton's iterational method. As the figure shows the value of strain ratio never reaches the critical limit " 10 " and therefore no solution can be obtained.

To overcome this problem and for the purpose of global convergence, a "backtracking" algorithm has been developed and added to the Newton's method. This special algorithm

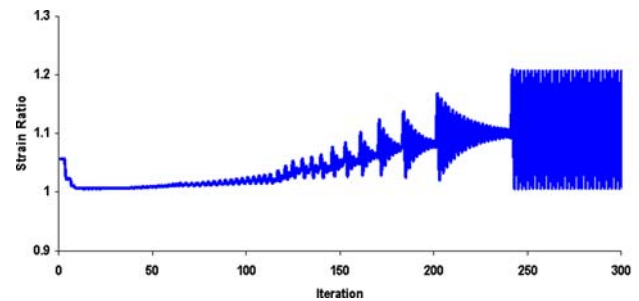


Fig. 2 The state of nonconverging problem in solution to FLD when Newton's method is applied alone

combines the rapid local convergence of Newton's method with a global-convergent strategy that will guarantee some progress toward the solution at each iteration. Based on this concept, Eq (24) is changed to the following form:

$$\mathbf{x}_{\text{new}} = \mathbf{x}_{\text{old}} + \lambda \delta \mathbf{x} \quad 0 < \lambda \leq 1 \quad (\text{Eq 26})$$

where λ is the step size and the vector $\delta \mathbf{x}$ is the direction of Newton's step. The aim in the backtracking algorithm is to find acceptable λ . It is required to identify a criterion which the convergence can be investigated. For this purpose, the function g is defined as follows:

$$g = \mathbf{F} \cdot \mathbf{F} \quad (\text{Eq 27})$$

To find an acceptable λ , it is required the function g decreases by Newton's steps. In every solution to (19), there may be local minima of (27) that are not solutions to (19). In this article the strategy of finding λ has been improved as follow:

$$\nabla g \cdot \delta \mathbf{x} = (\mathbf{F} \cdot \mathbf{J}) \cdot (-\mathbf{J}^{-1} \cdot \mathbf{F}) = -\mathbf{F} \cdot \mathbf{F} < 0 \quad (\text{Eq 28})$$

Due to the descent direction of the Newton's step, finding an acceptable step is guaranteed by backtracking along the Newton's step. The goal of backtracking algorithm is to move to a new point \mathbf{x}_{new} with the step size λ along the direction of the Newton's step $\delta \mathbf{x}$ so that $g(\mathbf{x}_{\text{old}} + \lambda \delta \mathbf{x})$ decreases sufficiently. The backtracking algorithm has been accomplished as follows: first select $\lambda = 1$ as the full Newton's step. This will lead to convergence when \mathbf{x} is sufficiently close to the solution. However, $g(\mathbf{x}_{\text{old}} + \lambda \delta \mathbf{x})$ must meet the acceptance criteria. For this case, Armijo (Ref 17) believes that the rate of decrease of $g(\mathbf{x})$, i.e. $g(\mathbf{x}_{\text{new}}) - g(\mathbf{x}_{\text{old}})$, to be at least some fraction γ of $\nabla g(\mathbf{x}) \cdot \delta \mathbf{x}$. Therefore, the condition for finding the optimum solution can be described by the following relation:

$$g(\mathbf{x}_{\text{new}}) \leq g(\mathbf{x}_{\text{old}}) + \gamma \nabla g(\mathbf{x}) \cdot (\mathbf{x}_{\text{new}} - \mathbf{x}_{\text{old}}) \quad (\text{Eq 29})$$

The parameter γ ranges between 0 and 1. Typically, small value of γ , for example $\gamma = 10^{-4}$ is a good selection (Ref 18). If $g(\mathbf{x}_{\text{old}} + \lambda \delta \mathbf{x})$ does not meet the proposed criteria, a smaller value of λ is selected. Based on the above explanation, a practical backtracking algorithm can be described as follow:

$$h(\lambda) = g(\mathbf{x}_{\text{old}} + \lambda \delta \mathbf{x}) \quad (\text{Eq 30})$$

Therefore,

$$h'(\lambda) = \nabla g \cdot \delta \mathbf{x} \quad (\text{Eq 31})$$

The algorithm starts with $h(0)$ and $h'(0)$ which are available. The first step is always the Newton's step, $\lambda = 1$. If this step is not acceptable, $h(1)$ is available as well. Considering $h(\lambda)$ as a quadratic function:

$$h(\lambda) = [h(1) - h(0) - h'(0)]\lambda^2 + h'(0)\lambda + h(0) \quad (\text{Eq 32})$$

Taking the derivative of this quadratic function shows there is a minimum when:

$$\lambda = \frac{-h'(0)}{2[h(1) - h(0) - h'(0)]} \quad (\text{Eq 33})$$

On the second and subsequent backtracks, h as a cubic in λ is modeled.

$$h(\lambda) = a\lambda^3 + b\lambda^2 + h'(0)\lambda + h(0) \quad (\text{Eq 34})$$

Using the previous value $h(\lambda_1)$ and the second most recent value $h(\lambda_2)$ provide two equations to obtain constants a and b :

$$\begin{bmatrix} a \\ b \end{bmatrix} = \frac{1}{\lambda_1 - \lambda_2} \begin{bmatrix} \frac{1}{\lambda_1^2} & -\frac{1}{\lambda_2^2} \\ -\frac{\lambda_2}{\lambda_1^3} & \frac{\lambda_1}{\lambda_2^3} \end{bmatrix} \begin{bmatrix} h(\lambda_1) - h'(0)\lambda_1 - h(0) \\ h(\lambda_2) - h'(0)\lambda_2 - h(0) \end{bmatrix} \quad (\text{Eq 35})$$

The minimum of the cubic (34) is at

$$\lambda = \frac{-b + \sqrt{b^2 - 3ah'(0)}}{3a} \quad b \leq 0 \quad (\text{Eq 36})$$

when $b > 0$ the minimum of the cubic (34) is at

$$\lambda = \frac{-h'(0)}{b + \sqrt{b^2 - 3ah'(0)}} \quad b > 0 \quad (\text{Eq 37})$$

If $a = 0$ the minimum is obtained from the following formula:

$$\lambda = -\frac{h'(0)}{2b} \quad (\text{Eq 38})$$

When the backtracking algorithm is applied to the FLD prediction process, the nonconvergence problem of Newton's method is eliminated. Figure 3 shows how the nonconverging problem in Fig. 2 is eliminated when the backtracking algorithm is applied to the Newton's method.

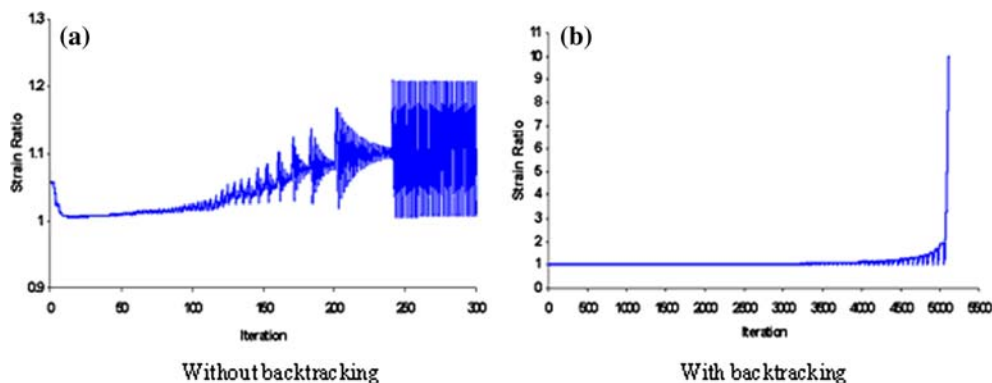


Fig. 3 Effects of backtracking algorithm on converging of the solution to the nonlinear formulations in FLD

6. Results and Discussions

To examine the capability of the developed algorithm in the Newton's method, prediction of FLD in AK steel has been selected as the case study. The adopted yield function in this work is BBC2000 (Ref 19). The formulation of this function can be written as follows:

$$\bar{\sigma}_y(a, b, c, M, N, P, Q, R, k, \sigma_{ij}) = \left[a \cdot (b\Gamma + c\Psi)^{2k} + a \cdot (b\Gamma - c\Psi)^{2k} + (1-a) \cdot (2c\Psi)^{2k} \right]^{1/2k} \quad (\text{Eq 39})$$

$$\Gamma = M\sigma_{11} + N\sigma_{22},$$

$$\Psi = \sqrt{(P\sigma_{11} + Q\sigma_{22})^2 + R\sigma_{12}\sigma_{21}}. \quad (\text{Eq 40})$$

where $a, b, c, M, N, P, Q, R, k$ are anisotropy coefficients. The material constants describing the yield function and hardening law for AK steel are shown in Tables 1 and 2.

Figure 4 shows the FLD of AK steel. The value of imperfection factor has been selected as 0.9990. As shown in Fig. 4, the FLD in the left-hand side is almost linear. The left-hand side of FLD and FLD° are independent of selection of yield function. This is due to act of σ_1 when σ_2 and σ_3 are almost negligible. In another word, the left-hand side of Fig. 4 is very close to the uniaxial tension test. Where, σ_2 and σ_3 are so little and their relations with σ_1 are not significant. Which means the result is not very sensitive to the yield function. But we have found the right-hand side of FLD enormously depends on the selection of yield function.

In fact, Fig. 2 shows the process of calculating one point of FLD in AK steel when the backtracking algorithm has not been applied to the FLD solution. Applying the backtracking algorithm increases the number of iterations. For example, by considering Fig. 3, for the same point on FLD about 5100 iterations are needed to reach the solution.

As mentioned, for obtaining one point of FLD, it is required to consider all groove angles between 0° and 90° . The limit strain as a candidate point on FLD is the minimum of all calculated limit strains for all groove angles. As shown in Fig. 5, on right-hand side of FLD, the candidate limit strains occur at zero groove angles. It means for computation of limit strain at right-hand side of FLD, it is enough to accomplish the calculation only for zero groove angles. In this case the groove direction is normal to the rolling direction. But on the left-hand side of FLD, depends on the material constants, local neck occurs at zero extension. At this direction, one of the nonshear strain components becomes zero.

Table 1 The material constants describing the hardening law

Material	K (MPa)	ε_0	n	m
AK Steel	426.2	0.00173	0.228	0.015

Table 2 The material constants describing the yield function

Material	a	b	c	k	M	N	P	Q	R
AK Steel	0.645	0.867	0.771	3	0.468	0.434	0.729	-0.712	1.81

The components of strain tensor at groove direction are obtained as follows:

$$\begin{bmatrix} \varepsilon_{11} & \varepsilon_{12} \\ \varepsilon_{12} & \varepsilon_{22} \end{bmatrix} = \begin{bmatrix} \cos \theta & -\sin \theta \\ \sin \theta & \cos \theta \end{bmatrix}^T \begin{bmatrix} \varepsilon_1 & 0 \\ 0 & \varepsilon_2 \end{bmatrix} \begin{bmatrix} \cos \theta & -\sin \theta \\ \sin \theta & \cos \theta \end{bmatrix}$$

$$= \begin{bmatrix} \varepsilon_1 \cos^2 \theta + \varepsilon_2 \sin^2 \theta & (\varepsilon_2 - \varepsilon_1) \sin \theta \cos \theta \\ (\varepsilon_2 - \varepsilon_1) \sin \theta \cos \theta & \varepsilon_2 \cos^2 \theta + \varepsilon_1 \sin^2 \theta \end{bmatrix} \quad (\text{Eq 41})$$

Zero extension occurs when $\varepsilon_{22} = 0$, i.e.

$$\varepsilon_2 \cos^2 \theta + \varepsilon_1 \sin^2 \theta = 0 \quad (\text{Eq 42})$$

or,

$$\tan \theta = \sqrt{-\frac{\varepsilon_2}{\varepsilon_1}} = \sqrt{-\rho} \quad (\text{Eq 43})$$

This angle shows the direction of zero extension. Thus the FLD calculation procedure for left- and right-hand sides

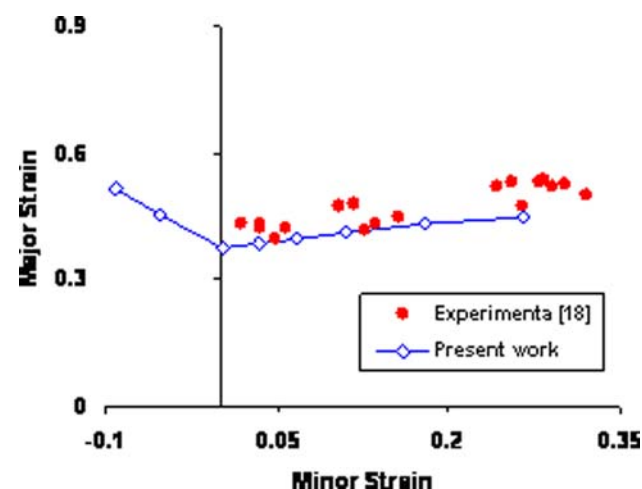


Fig. 4 Comparison of the predicted FLD with the experimental results (Ref 15) in AK steel

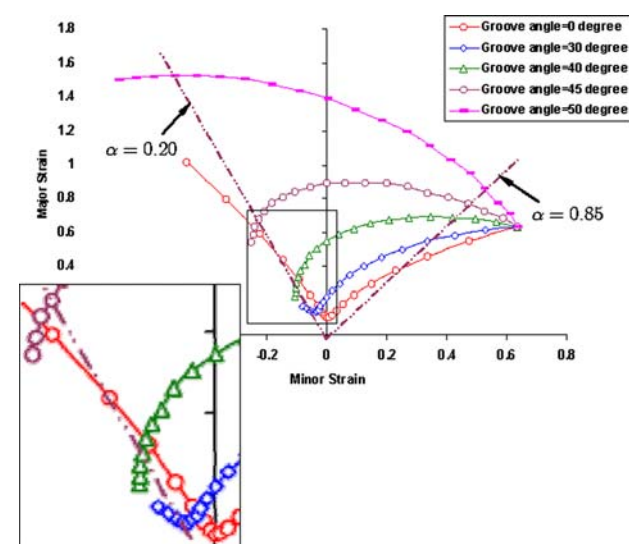


Fig. 5 Effect of groove orientation on the prediction of FLD

are simplified. On the right-hand side of FLD, limit strains are obtained for zero groove angles. On the left-hand side of FLD with specified strain path ρ , first the groove angle is calculated and then the limit strain for this angle is obtained.

7. Summary

In this article, to predict the FLD, “Marciniak and Kuczynski” model has been used. The numerical technique used for solution of the nonlinear equations is Newton’s method. To eliminate the nonconverging problem of the Newton’s method, a particular backtracking algorithm has been developed and implemented. This algorithm guaranteed the convergence of solution. Applying this algorithm to the FLD formulation, the numerical process becomes very robust which can be used for any types of yield functions. Among the yield functions, for the case of AK steel, BBC2000 resulted an FLD with good agreement with the experimental results. Also the necking direction on the left- and right-hand sides of FLD appears with different angles. For all limit strains at the right-hand side of FLD, necking occurs at zero groove angles. But any limit strain at the left-hand side of FLD depends on the strain path.

References

1. S.P. Keeler, Circular Grid System: A Valuable Aid for Evaluation Sheet Forming, *Sheet Met. Ind.*, 1969, **45**, p 633–640
2. G.M. Goodwin, Application of Strain Analysis to Sheet Metal Forming Problems, *Metall. Ital.*, 1969, **60**, p 767–771
3. Z. Marciniak and K. Kuczynski, Limit Strains in the Process of Stretch-Forming Sheet Metal, *Int. J. Mech. Sci.*, 1967, **9**, p 609–620
4. Z. Marciniak, K. Kuczynski, and T. Pokora, Influence of the Plastic Properties of a Material on the Forming Limit Diagram for Sheet Metal in Tension, *Int. J. Mech. Sci.*, 1973, **15**, p 789–805
5. J. Slota and E. Spisak, Comparison of the Forming Limit Diagram (FLD) Models for Drawing Quality (DQ) Steel Sheets, *METABK*, 2005, **44**(4), p 249–253
6. D. Banabic, H. Aretz, L. Paraianu, and P. Jurco, Application of Various FLD Modeling Approaches, *Model. Simul. Mater. Sci. Eng.*, 2005, **13**, p 759–769
7. D. Banabic and E. Dannenmann, Prediction of the Influence of Yield Locus on the Limit Strains in Sheet Metals, *J. Mat. Proc. Tech.*, 2001, **109**, p 9–12
8. H.M. Huang, J. Pan, and S.C. Tang, Failure Prediction in Anisotropic Sheet Metals Under Forming Operations with Consideration of Rotating Principal Stretch Directions, *Int. J. Plast.*, 2000, **16**, p 611–633
9. M. Kuroda and V. Tvergaard, Forming Limit Diagrams for Anisotropic Metal Sheets with Different Yield Criteria, *Int. J. Solids Struct.*, 2000, **37**, p 5037–59
10. J. Cao, H. Yao, A. Karafillis, and M.C. Boyce, Prediction of Localized Thinning in Sheet Metal Using a General Anisotropic Yield Criterion, *Int. J. Plast.*, 2000, **16**, p 1105–1129
11. A. Parmar and P.B. Mellor, Predictions of Limit Strains in Sheet Metal Using a More General Yield Criterion, *Int. J. Mech. Sci.*, 1978, **20**, p 385–391
12. S. Xu and K.J. Weinmann, Prediction of Forming Limit Curves of Sheet Metals Using Hill’s 1993 User-Friendly Yield Criterion of Anisotropic Materials, *Int. J. Mech. Sci.*, 1998, **40**(9), p 913–925
13. H. Yao and J. Cao, Prediction of Forming Limit Curves Using an Anisotropic Yield Function Prestrain Induced Backstress, *Int. J. Plast.*, 2002, **18**, p 1013–1038
14. M.C. Butuc, A.B. da Rocha, J.J. Gracio, and J.F. Duarte, A More General Model for Forming Limit Diagrams Prediction, *J. Mater. Process. Technol.*, 2002, **125–126**, p 213–18
15. M.C. Butuc, D. Banabic, A.B. da Rocha, J.J. Gracio, J.F. Duarte, P. Jurco, and D.S. Comsa, The Performance of Yld96 and BBC2000 Yield Functions in Forming Limit Prediction, *J. Mater. Process. Technol.*, 2002, **125–126**, p 281–286
16. C. Woodford and C. Phillips, *Numerical Methods with Worked Examples*. Chapman & Hall, London, UK, 1997, 35–58 (Chapter 2)
17. L. Armijo, Minimization of Functions having Lipschitz Continuous First Partial Derivatives, *Pacific J. Math.*, 1966, **6**, p 1–3
18. W.H. Press, S.A. Teukolsky, W.T. Vetterling, and B.P. Flannery, *Numerical Recipes in Fortran 77: The Art of Scientific Computing*. Press Syndicate of the University of Cambridge, Cambridge, 1992 (Chapter 9)
19. F. Barlat and J. Lian, Plastic Behavior and Stretchability of Sheet Metals. Part I. A Yield Function for Orthotropic Sheet Under Plane Stress Conditions, *Int. J. Plast.*, 1989, **5**, p 51–56